Colloids and Surfaces A: Physicochem. Eng. Aspects 422 (2013) 81–89

Contents lists available at SciVerse ScienceDirect

Colloids and Surfaces A: Physicochemical and Engineering Aspects

journal homepage: www.elsevier.com/locate/colsurfa

Poly(ethylene glycol)-cross linked poly(methyl vinyl ether-co-maleic acid)hydrogels for three-dimensional human ovarian cancer cell culture

Tianzhu Zhang[a,b,*], Junsong Chen[c,1], Qiying Zhang[a,b,c], Jun Dou[c], Ning Gu[a,b]

[a] Jiangsu Key Laboratory for Biomaterials and Devices, State Key Laboratory of Bioelectronics, School of Biological Science and Medical Engineering, Southeast University, Sipailou 2, Nanjing 210096, China
[b] Suzhou Key Lab of Biomedical Materials and Technology, Research Institute of Southeast University in Suzhou, Ren Ai Road 150, Suzhou Industrial Park, Suzhou 215123, China
[c] Department of Pathogenic Biology and Immunology, Medical School, Southeast University, Dingjiaqiao 87, Nanjing 210009, China

HIGHLIGHTS

- Ovarian cancer cell line HO8910 can form multicellular spheroids (MCS) in PEG-cross linked PMVE-*co*-MA hydrogel.
- Elastic modulus G' of hydrogel can remarkably influence the proliferation of HO8910; the higher elastic modulus is more beneficial to the adhesion and proliferation of HO8910.
- PMVE-*co*-MA-based hydrogel is potential 3D cell culture matrix.

GRAPHICAL ABSTRACT

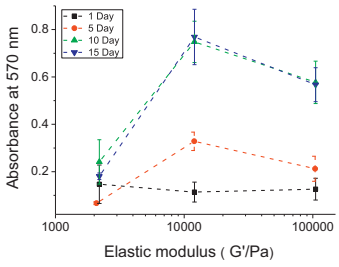

ARTICLE INFO

Article history:
Received 28 August 2012
Received in revised form 15 January 2013
Accepted 22 January 2013
Available online xxx

Keywords:
3D culture
Multicellular spheroid
Human ovarian cancer cell
Hydrogel
Poly(methyl vinyl ether-*co*-maleic acid)
Rheological properties

ABSTRACT

In this work, three kinds of poly(ethylene glycol)-cross linked poly(methyl vinyl ether-*co*-maleic acid) hydrogels, Gel-1, Gel-2, and Gel-3 with different elastic modulus of 105,100 Pa, 12,020 Pa, and 2191 Pa were designed for simulating respectively the mechanical strength of stiffer metastasis bone sites, cancerous soft tissue, and BME or collagen, and were evaluated in three-dimensional (3D) culture of human ovarian cancer cell line HO8910. The proliferation, adhesion, migration, and invasion of ovarian cells HO8910 in these three kinds of hydrogels were systematically investigated and compared with two commercial hydrogels BME and collagen I. Hydrogels Gel-1 and Gel-2 with higher elastic modulus showed a better cytocompatibility and remarkably supported the proliferation of ovarian cancer cell line HO8910 and the formation of multicellular spheroids (MCS) in a 3D model. The mechanical properties of hydrogels played a crucial role in responses of HO8910 cells. The hydrogels Gel-1 and Gel-2 are also the potential 3D culture matrix materials for cancer cell culture.

1. Introduction

Compared with the traditional two-dimensional (2D) cell cultures, the three-dimensional (3D) tumor cell culture is still attracting a lot of attentions, because it can provide more information about cancer, including tumorigenesis, proliferation, invasion, and distant metastases of cancer cells [1,2]. Especially, the 3D tumor cell culture has been widely used for high-throughput screening and evaluation of cytotoxic effect of chemotherapeutic drugs [3,4]. For 3D tumor cell cultures, the choosing of appropriate culture matrix materials similar to the key features of natural extracellular

* Corresponding authors at: Jiangsu Key Laboratory for Biomaterials and Devices, State Key Laboratory of Bioelectronics, School of Biological Science and Medical Engineering, Southeast University, Sipailou 2, Nanjing 210096, China.
Tel.: +86 0 25 83272476; fax: +86 0 25 83272460.
E-mail addresses: zhangtianzhuglq@yahoo.com.cn (T. Zhang), guning@seu.edu.cn (N. Gu).
[1] Co-first author.

0927-7757/$ – see front matter © 2013 Elsevier B.V. All rights reserved.
http://dx.doi.org/10.1016/j.colsurfa.2013.01.030

matrices (ECM) is very critical [5]. The commonly used natural matrix materials include collagen [6], chitosan [7], alginate [8], agar [9], Matrigel (BD Bioscience) [10], hyaluronic acid [11], gelatin [12], and their derivatives etc., which present good cytocompatibility and lower cytotoxicity and therefore are relatively easily processed to support the proliferation of cancer cell in 3D.

Due to the inherent disadvantages of these natural materials, such as batch-to-batch variability and containing of residual growth factors [13], many synthesized materials are being used as 3D matrix. The design flexibility of biochemical and biophysical characteristics of synthetic materials can overcome the limitation of naturally derived matrices, which will contribute to dismantle complex issues into some more simple and defined questions trackable in an in vitro controllable setting.

Epithelial ovarian cancer is often an aggressive disease, and usually was diagnosed only until it developed an advanced stage because of the underlying complex mechanism. At the late stage, the chemotherapy resistance often occurs. So, the 3D culture study aiming at the metastasis and multidrug resistance (MDR) of ovarian cancer are becoming more important and challenging. It was found that the construction of multicellular spheroids (MCS) of ovarian cancer cells is effective tools for the investigation of mechanism of the chemotherapy resistance [14,15].

The peptide nanofibers are a kind of excellent matrix materials [16,17]. Three different ovarian cancer cell lines A2780, A2780/DDP, and SK-OV-3 exhibited nearly similar adhesion and invasion behaviors in vitro between RADA16-I peptide nanofiber and type I collagen. The formed multicellular spheroids of A2780 and A2780/DDP and the cell clusters of SK-OV-3 had two-fold to five-fold higher anticancer drug resistance of 5-fluorouracil, paclitaxel, and curcumin than in 2D Petri dish culture [18].

Some hydrogels based multi-arm poly(ethylene glycol) (PEG) were synthesized and used in 3D ovarian cancer cell culture [19]. Rizzi et al. prepared different kind of PEG-based hydrogels, namely, RGD-functionalized hydrogel, non-RGD-functionalised hydrogels, matrix metalloproteases (MMP)-sensitive hydrogel, and MMP-insensitive hydrogel [20]. Two kinds of epithelial ovarian cancer cell lines (OV-MZ-6 and SKOV-3) were cultured in this PEG-based hydrogel. The proliferations of OV-MZ-6 and SKOV-3 cells are dependent on cell–integrin engagement and the ability of cells to proteolytically remodel their extracellular microenvironment. Cell spheroid grown in stiffer ($G' = 1201 \pm 121$ Pa) hydrogels proliferated less than in softer ($G' = 241 \pm 19$ Pa) hydrogels.

Besides the native interaction between cells and the chemical nature of materials influences the physiological processes of cells, the physical properties of materials will also lead to the significantly different behaviours of cells [21]. Although different materials were designed to study the behaviours of ovarian cancer, such as degradability of EMC and anticancer drugs resistance, the systematic investigation of influence of mechanical properties of different materials on the behaviours of ovarian cancer cells in 3D model is insufficient. In fact, the stiffness of ovarian cancer cells is also different. The stiffness of highly invasive ovarian cancer cells (HEY A8) is lower than that of their less invasive parental cells (HEY) [22]. It is extremely necessary to further probe the response of ovarian cancer cells to the different kind of hydrogels.

The aim of this work is to offer a cheap synthetic poly(methyl vinyl ether-*co*-maleic acid) (PMVE-*co*-MA)-based hydrogel suitable for ovarian cancer cells 3D culture and an insight into how the mechanical properties of this kind of hydrogel influence the formation of multicellular spheroids (MCS) of ovarian cancer cells. Here, we found PEG-cross linked PMVE-*co*-MA hydrogels could be used as matrices for culture of human ovarian cancer cell line HO8910, and HO8910 cells formed multicellular spheroids in this kind of hydrogel. The relation of elastic modulus of hydrogel and the formation of MCS were investigated, which can contribute to further understanding of the formation conditions of ovarian cancer MCS.

Table 1
The preparation formula, crosslinking degree, and elastic modulus of three PEG-cross linked PMVE-*co*-MA hydrogel samples.

Sample	r	$\overline{M}_c$	X	G'/Pa (at 37 °C)
Gel-1	140:1	23,200	5.4×10^{-5}	105,100
Gel-2	280:1	35,400	3.8×10^{-5}	12,020
Gel-3	790:1	78,600	8.0×10^{-6}	2,191

$r = n_{-COOH}:n_{-OH}$, molar ratio of carboxyl groups in PMVE-*co*-MA to hydroxyl groups in PEG; $\overline{M}_c = (r \times 174 + M_n)/2$, where 174 is molecular weight of the repeating unit in PMVE-*co*-MA, M_n is the number average molecular weight of PEG, M_n is 19,700 for PEG_{10K}, and M_n is 22,000 for PEG_{20K}.
X is the crosslinking degree, and is calculated as follows: $X = \frac{\rho}{M_c}$.
G' is the elastic modulus of hydrogel.

2. Materials and methods

2.1. Materials

Poly (methyl vinyl ether-*co*-maleic anhydride) (PMVE-*co*-MAH) (M_w = 1,080,000, M_n = 311,000, *MDW* = 3.47) and 3-(4,5-dimethylthiazol-2-yl)-2,5-diphenyl tetrazolium bromide (MTT) were purchased from Sigma–Aldrich (Shanghai, China). Poly(ethylene glycols) (PEG_{10K}: M_w = 24,800, M_n = 19,700, *MDW* = 1.26; PEG_{20K}: M_w = 29,400, M_n = 22,000, *MDW* = 1.34) and sodium hydrogen carbonate ($NaHCO_3$) were obtained from Sinopharm Chemical Reagent Shanghai Co. Ltd. The human ovarian cancer cell line HO8910 were purchased from the cell bank of Chinese Academy of Sciences in Shanghai. BME and collagen I gel were purchased from Trevigen Inc. Other reagents are commercially available.

2.2. Preparations of hydrogels and hydrogel dispersions

0.7800 g PMVE-*co*-MAH was added to 20 mL deionized water in a 100 mL round-bottom flask and heated at 90 °C to hydrolyze for 2 h to obtain a clear solution of poly (methyl vinyl ether-*co*-maleic acid) (PMVE-*co*-MA) with vigorous stirring. The required amount of PEG, 0.7812 g PEG_{20K} for Gel-1, 0.3913 g PEG_{20K} for Gel-2, and 0.1253 g PEG_{10K} for Gel-3, was added to the above PMVE-*co*-MA aqueous solution to obtain the uniform mixture of PEG and PMVE-*co*-MA, and then the water was removed with a rotary evaporator and cured at 80 °C for 24 h in a beaker to induce the esterification reaction between PEG and PMVE-*co*-MA for the formation of gel. Finally, three kinds of hydrogel films were obtained for ATR-FTIR and reological analysis. The preparation formulas of three kinds of hydrogels were listed in Table 1. The obtained dried hydrogel were ground down into fragments, then hydrogel fragments were dissolved in the deionized water and saturated $NaHCO_3$ aqueous solution was added to obtain 2.0 wt% hydrogel dispersion with pH 7.2. The equilibrium time of pH value of hydrogel dispersion to reach 7.2 needs at least a week. The density (ρ) of the polymeric films was calculated by using the following formula: $\rho = W/SD$, where W is the weight of the film, D is the thickness of the film, and S is the cross-sectional area.

2.3. ATR-FTIR spectra analysis

The attenuated total reflectance Fourier transform infrared (ATR-FTIR) spectra were obtained using a Nicolet 5700 spectrometer (Thermo, U.S.A.) with a Wilks model 10 ATR accessory at an angle of 45° using a KRS-5 crystal. Spectra were recorded at 4 cm^{-1} resolution between 4000 and 400 cm^{-1} and were the sum of 256 individual scans.

2.4. Interior morphology observation by scanning electron microscopy (SEM)

SEM measurements of three kinds of hydrogel samples were performed to investigate their interior morphology. Hydrogel samples were first swollen to equilibrium in distilled water at room temperature, quickly frozen in liquid nitrogen thereafter, and further freeze-dried in a Freezone 6 freeze drier (Labconco Corporation, USA) under vacuum at –42 °C for at least 48 h until all the solvent was sublimed. For SEM measurement, freeze-dried hydrogels were sectioned carefully and coated with gold; their interior morphology was studied with the scanning electron microscope (LEO, 1530VP, Germany).

2.5. Rheological characterization

Before measurement, three kinds of hydrogel films were swollen fully with distilled water to equilibrium state. Then the swollen hydrogel films were the neutralized with saturated $NaHCO_3$ aqueous solution until the pH 7.2. The concentration of fully swollen hydrogels Gel-1, Gel-2, and Gel-3 is 2.58%, 8.27%, and 3.29%, respectively. The dynamic rheological behavior of three kinds of hydrogel films was characterized with a HAAKE RheoStree 600 rheometer (Thermo Haake, Germany), equipped with a parallel plate of 35 mm in diameter. The sample gap was set to be 1.0 mm. The temperature sweeping were monitored to characterize the viscoelastic properties (elastic (G') and loss (G'') moduli) with heating rate of 1 °C/min and the frequency of 10 rad/s. The strain amplitude of 1% was kept to ensure a linear viscoelastic region.

2.6. HO8910 cells culture in hydrogels (3D on-top assay)

a) Cell proliferation assay: The employed culture method is the 3D on-top assay. Cell dispersion with a concentration of 8×10^4 cells/mL was first mixed with equal volume of 5 wt% hydrogel dispersion. To each well of a 96-well culture plate, 50 μL hydrogel dispersion was added and incubated at 37 °C for 1 h to obtain a stable hydrogel layer. Then 100 μL cell suspensions were added slowly on the hydrogel layer, followed by the subsequent addition of culture medium consisting of Dulbecco's Modified Eagle Medium (DMEM), 10% heat inactivated fetal bovine serum (FBS), 1% penicillin, and streptomycin admixture. The 96-well culture plate was maintained in an incubator at 37 °C with a humidified atmosphere of 5% CO_2. The culture medium was replaced every 2 days. The morphology of the cells cultured in the matrices was observed by a Plympus LX70–140 microscope. The proliferation of ovarian cancer cells in hydrogel was measured using MTT assay. After cultured for a given period, the cells were incubated with 20 μL 3-(4,5-dimethylthiazol-2-yl)-2,5-diphenyltetrazolium bromide (MTT) solution (5 mg/mL) for 4 h in the incubator at 37 °C. 50 μL DMSO were added to dissolve the formed formazan crystals. The Ultra-vis absorbance of formazan crystals solution was measured spectrophotometrically at 570 nm to determine the number of living cells.

b) Cell adhesion assay: 50 μL hydrogel was added into well of 96-well flat-bottom poly (vinyl chloride) (PVC) plate. A control well was coated with 200 μL solution of 10 mg/mL BSA. Then the plate was incubated at 4 °C for 1 h to get stable hydrogel layer. Then per well was added with 50 μL cell suspension with 10,000 cells respectively and cultured at 37 °C for 4 h, carefully pipette off the suspension of cells, and rinsed twice with PBS solution. Then 20 μL MTT solution (5 mg/mL) and 50 μL DMSO were added respectively as the above procedure.

c) The Migration and invasion assay: Establish the Transwell using Millicell-polycarbonate (PCF) insert (Millipore, Billerica, MA, USA). Coated the basement membrane PCF with 35 μL hydorgel dispersion to obtain a hydrogel layer, then added 100 μL cell suspension to the formed hydrogel layer, 10,000 cells were hold in per well, cultured at 37 °C for 24 h. 24 h later, the cells in hydrogel and hydrogel were first removed gently with a cotton swab, rinsed with PBS twice. The adhered cells to the PCF membrane were fixed with 4.0% formaldehyde, stained with 0.4% Trypan blue violet, and the number of cell was counted under the optical microscope.

All the above three assays were carried out in triplicate to obtain an average value. Data are expressed as mean ± standard error. Results for all analyses with a P value <0.05 indicated the statistically significant differences (* $P < 0.05$). It was determined using either two tailed unpaired t-tests or Mann–Whitney U test for nonparametric data.

3. Results and discussion

3.1. Synthesis and morphology characterization of hydrogel

The crosslinking reaction of PEG and PMVE-*co*-MA was performed through heating at 80 °C for 24 h (Scheme 1). Two cross linkers, PEG_{20K} and PEG_{10K}, were used in the crosslinking reaction. Here, three different ratios of carboxyl groups of PMVE-*co*-MA to hydroxyl groups of PEG, namely, 140:1, 280:1, and 790:1, were used respectively to obtain sample Gel-1, Gel-2, and Gel-3, which means that per carbonyl (>C═O) in ester group is theoretically connected at two sides with a 140, 280, and 790 repeating units length of PMVE-*co*-MA on average, respectively.

Fig. 1 shows the ATR-FTIR spectra of three samples. According to the previous report [23],the absorption band of ester carbonyl is 1730 cm^{-1} while the absorption band of carbonyl in the carboxylic acid group is 1708 cm^{-1}. In Fig. 1, from Gel-1, Gel-2, to Gel-3, with the decreasing crosslinking degree, the absorption bands of carbonyl (>C═O) in ester group and carboxylic acid obviously gradually changed. For Gel-1 with an higher crosslinking degree, the absorption band for carbonyl in ester group is remarkably at 1730 cm^{-1}, no absorption band of carbonyl groups in carboxylic acid were observed. This is because that the strong absorption of carbonyl in the ester groups completely covered that of carbonyl of carboxylic acid. With the decreasing crosslinking degree, for example, for Gel-3, not only was the absorption bands of carbonyl in ester groups observed, but also the absorption band of carbonyl in nonreacted carboxylic acids was observed at 1708 cm^{-1}. The sample Gel-1 shows an overlapped absorption band from two different kinds of carbonyl groups. These results indicates that the esterifiction reaction did occurred with the addition of cross linker PEG, moreover, not all of the acid groups reacted with the hydroxyl groups on the PEG molecules.

The IR measurement results are consistent with that reported previously [24].

The theoretical number average molecular weight $\overline{M}_c$ between two adjacent crosslinking points of sample Gel-1, Gel-2, and Gel-3 is 23,200, 35,400, and 78,600, respectively. $\overline{M}_c$ is calculated as follows:

$$\bar{M}_c = \frac{r \times 174 + M_n}{2} \quad (1)$$

where 174 is molecular weight of the repeating unit (MVE and MA) in PMVE-*co*-MA, M_n is the number average molecular weight of PEG, M_n is 19,700 for PEG_{10K}, and M_n is 22,000 for PEG_{20K}; r is n_{-COOH}:n_{-OH}, molar ratio of carboxyl groups in PMVE-*co*-MA to hydroxyl groups in PEG.

The crosslinking degree (X) is inversely proportional to $\overline{M}_c$, and X is calculated as follows:

$$X = \frac{\rho}{\overline{M}_c} \quad (2)$$

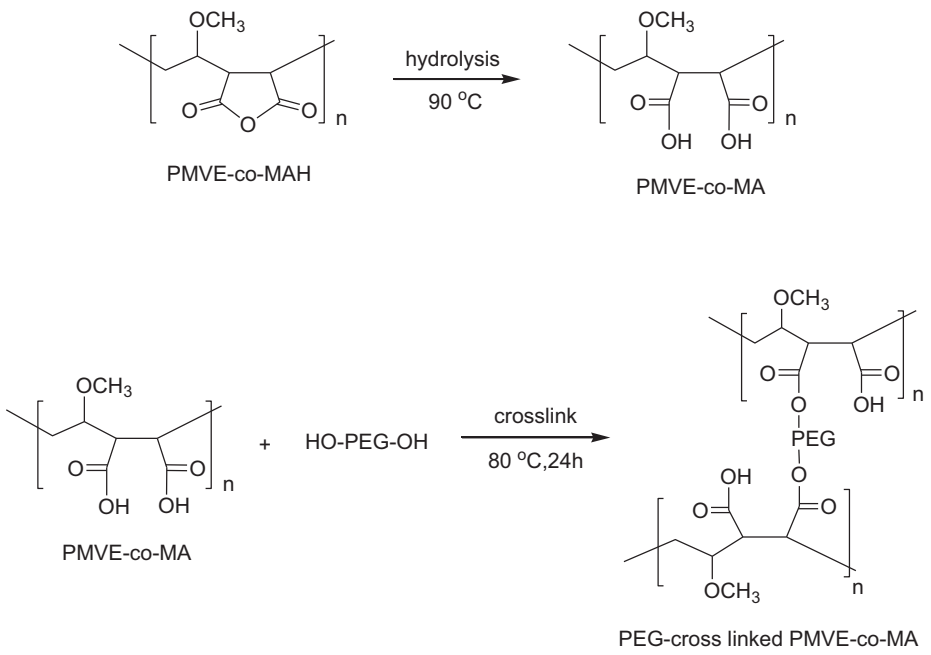

Scheme 1. Crosslinking reaction of PMVE-*co*-MA with PEG.

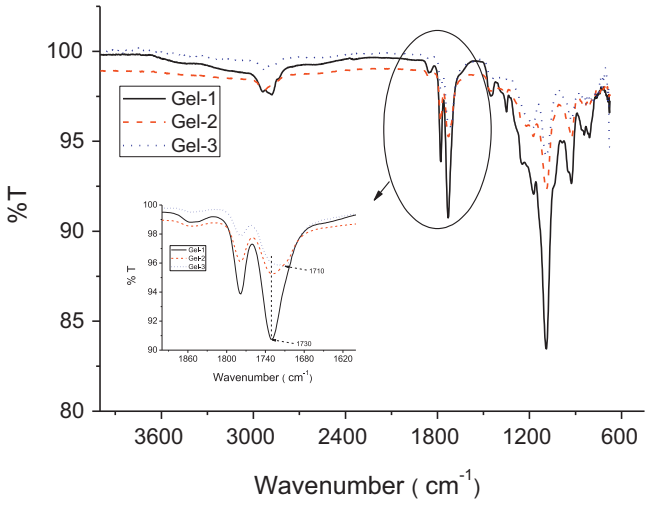

Fig. 1. ATR-FTIR spectra of three kinds of hydrogels Gel-1, Gel-2, and Gel-3.

Therefore, X means the number of effective network chains per unit volume. ρ (g/cm^3) is the density of polymer, the determined density of Gel-1, Gel-2, and Gel-3 is 1.2476 g/cm^3, 1.3442 g/cm^3, and 0.6274 g/cm^3, respectively. From sample Gel-1, via Gel-2 to sample Gel-3, the crosslinking degree decreases gradually (Table 1).

In Fig. 2, A_1, A_2 and A_3 show the porous structure of hydrogel Gel-1, Gel-2 and Gel-3, respectively. With the decreasing crosslinking degree (X), the porosity of hydrogel increases gradually. The irregular narrower strips structure is typical morphology of Gel-1 in A_1, in Gel-2, besides narrower strips structure, some wider strip structure was also found, for Gel-3, there are mainly slice-like structures in A_3. After ground, these porous structures of hydrogel were destroyed and subsequently nearly similar irregular pieces, namely hydrogel microparticles, were formed (Fig. 2, B_1–B_3), which can be conveniently transferred with a pipette to the culture plates.

3.2. Rheological analysis

At 37 °C, the elastic modulus G' of hydrogel films Gel-1, Gel-2 and Gel-3 is 105.1 kPa, 12.0 kPa, and 2.2 kPa, respectively. The rheological moduli of three kinds of samples are nearly independent on the temperature within the temperature sweeping range of 25–37 °C. (Fig. 3). The mean G' of hydrogel films Gel-1, Gel-2 and Gel-3 is respectively is 104.2 kPa, 12.0 kPa, 2.0 kPa. The stiffness of hydrgel increases with the crosslinking degree (X). This is to say, with the increase of X, the $\overline{M}_c$ will decrease and can lead to a higher network density, so the elasticity of hydrogel will increase. It was reported that Matrigel and collogen matrices exhibit a weaker mechanical strength (E = 0.1–10 kPa) and the cancerous soft tissue has a higher range elasticities (E = 1–100 kPa), while the common metastasis bone site has a much higher E ($\gg$100 kPa) [25]. Therefore, only through adjusting the crosslink degree, the very different elastic modulus can be obtained. Here, Gel-1, Gel-2, and Gel-3 simulate respectively the mechanical properties of Matrigel or collagen, cancerous soft tissue, and stiffer metastasis bone sites to some extent.

3.3. Proliferation of human ovarian cancer cells in hydrogel

As a polyanion electrolyte, PMVE-*co*-MA also shows a better cytocompatibility. However, during the cell culture, it was found that the pH value of hydrogel is critical to the growth of cells. For the support of cell growth, pH value should be kept neutral or slightly basic, here pH value is 7.2. Too lower or too higher pH value is detrimental for cell growth.

Three kinds of hydrogels with the different elastic modulus G' show the different 3D culture results of HO8910 cells (Fig. 4). In Gel-1 and Gel-2, the cells grow slowly in the first five days. From 10th day to 15th day, the proliferation of HO8910 cells leveled off. If linearly fitting the absorbance (y) (570 nm) and time (x) (day) (1–15 day), two equations were obtained: for Gel-1, $y = 0.09258 + 0.03589\,x$ (correlation factor $R = 0.9269$), and for Gel-2, $y = 0.09892 + 0.05043\,x$ (correlation factor $R = 0.9503$). So, HO8910 cells grew faster in hydrogel Gel-2 than in other two hydrogels

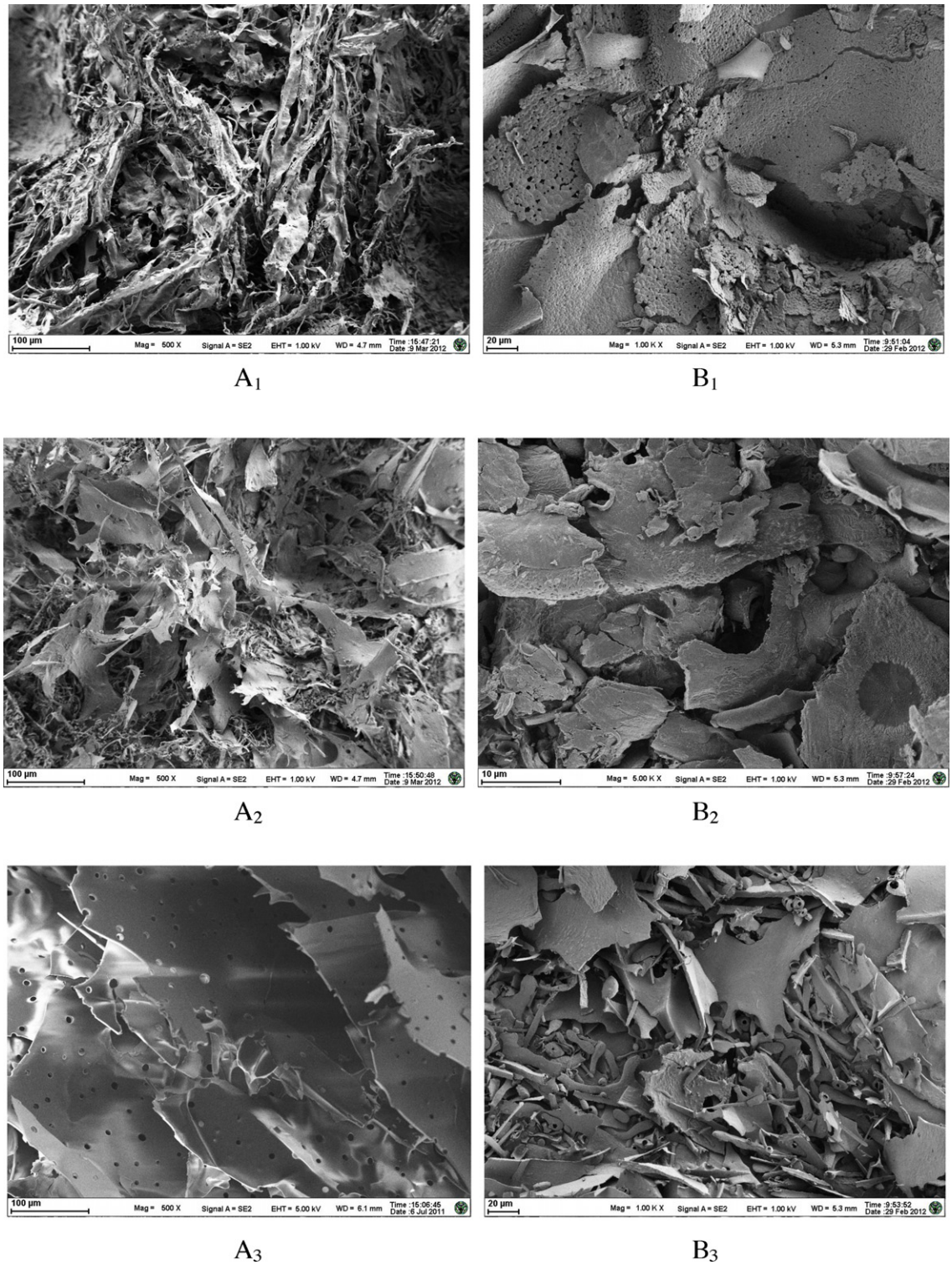

Fig. 2. SEM images of the cross section of hydrogel Gel-1 (A_1 and B_1), Gel-2 (A_2 and B_2) and Gel-3 (A_3 and B_3). Before ground (A_1–A_3); after ground (B_1–B_3).

Gel-1 and Gel-3. Compared with the cell proliferation in hydrogel Gel-1 and Gel-2, ovarian cancer cells show the lower proliferation viability in hydrogel Gel-3. It was also found the number of viable HO8910 cells decreased on 20th day as previously reported. The possible reason is that oxygen and other nutrient supply by passively diffusion can not meet the demand of continuously growing MCS, similar to the culture results of HepG2 in hydrogel [26].

Fig. 5 shows the typical proliferation of HO8910 cells in the hydrogel Gel-2. On the fifth day (Fig. 5a), HO8910 cells aggregated loosely to form colonies, on the tenth-fifteenth day, the structure of cell aggregates not only became more compact, but also the number of cell aggregates increased, the obvious 3D multicellular spheroids were formed with a size of some 200 μm (Fig. 5b and c). On the twentieth day, the number of cells aggregates did not increase any more and the proliferation

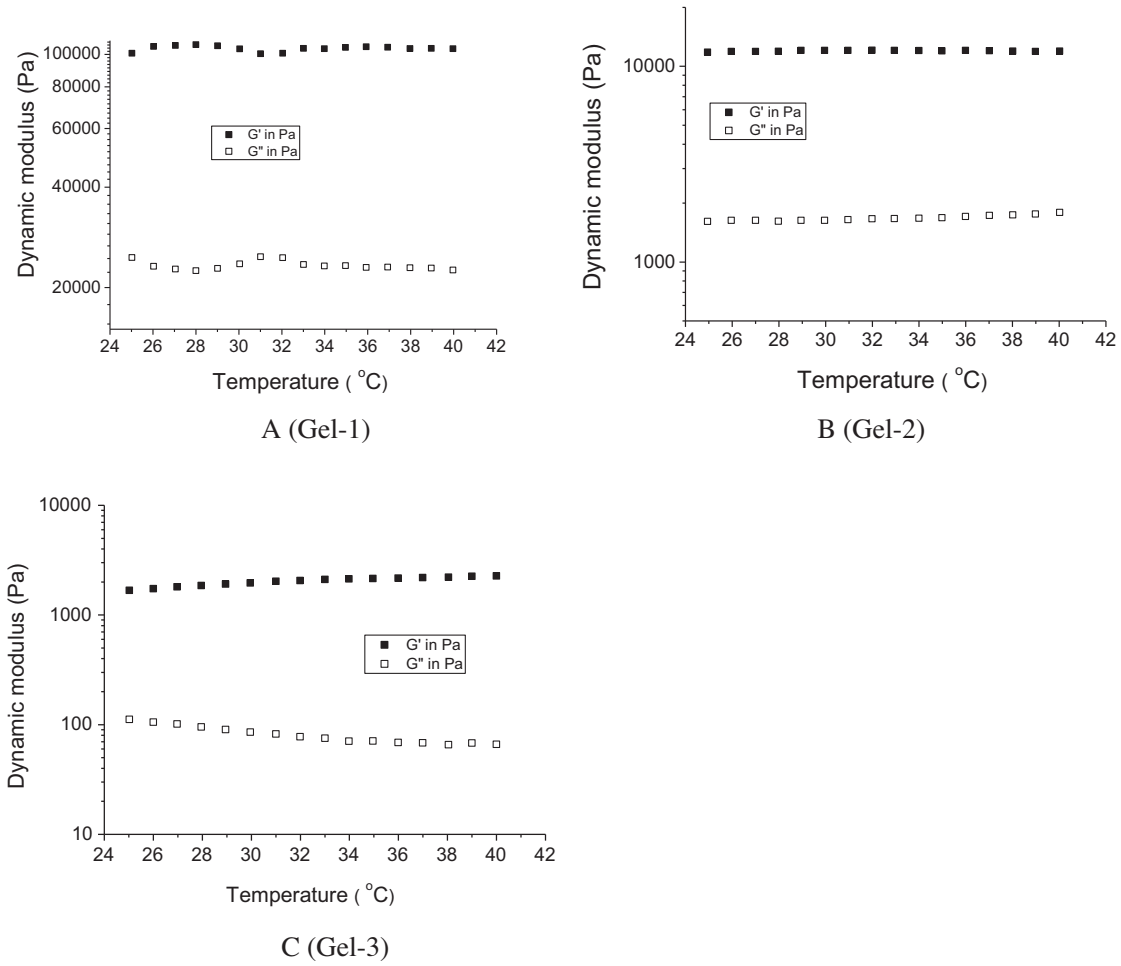

Fig. 3. Elastic modulus G' and viscous modulus G'' of Gel-1, Gel-2, and Gel-3 at the different temperature with the strain of 1% and the frequency of 10 rad/s.

activity of cell started to decrease. Fig. 4 gave more quantitative evidences.

3.4. Adhesion of human ovarian cancer cells on hydrogel

Generally speaking, the adhesion of cancer cells on the matrices is the first step for the formation of MCS, so the cell–hydrogel interaction is a very crucial determinant for the formation of MCS. Therefore, the adhesion behaviors of HO8910 cells on these three kinds of hydrogels were investigated here; the obtained results were compared with that of commercial hydrogel BME and collagen I.

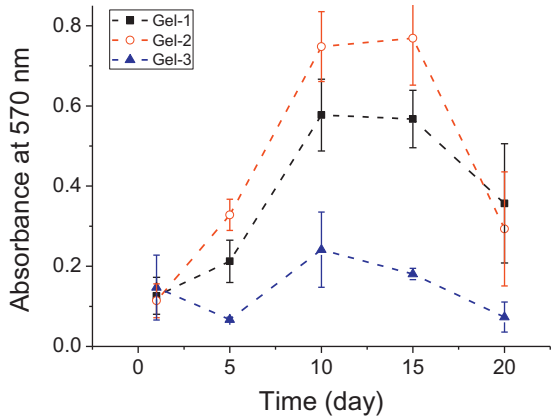

Fig. 4. Proliferation of HO8910 cells cultured in Gel-1, Gel-2 and Gel-3 hydrogels as assessed by MTT assays. (All images were captured at ×100 magnification; Scale bar: 100 μm).

The hydrogel Gel-2 shows the best cell adhesion capability among Gel-1, Gel-1 and Gel-3 for HO8910 cells, the absorbance at 570 nm of Gel-2 is 0.3970, 32.3% higher than that of Gel-1, 51.0% higher than that of Gel-3. Even compared with commercial hydrogels BME and collagen I, the hydrogel Gel-2 presents the nearly same cell adhesion capability too, the absorbance of Gel-2 is 5.3% slightly higher than that of BME, 25.7% higher than that of collagen I. The hydrogel Gel-3 shows the lowest cell adhesion capability, the absorbance of Gel-3 is only 0.263, slightly higher than that of BSA (Fig. 6).

Fig. 7 show the optical pictures of adhered cells on the different hydrogels. The number of adhered cells on Gel-2 is similar to that of collagen I, bigger than that of Gel-1, and much bigger than that of Gel-3 and BSA. Combing with Fig. 6, we can clearly score the cell adhesion capability of three synthesized hydrogels. Namely, Gel-2 > Gel-1 > Gel-3. As a whole, the adhesion capability of synthetic hydrogel increases with the storage modulus. This adhesion assay can interpret well the proliferation of HO8910 cells in these three kinds of hydrogels.

3.5. Migration and invasion of the ovarian cancer cells

The migration and invasion of ovarian cells in the synthesized hydrogel can be used as important criteria to evaluate whether

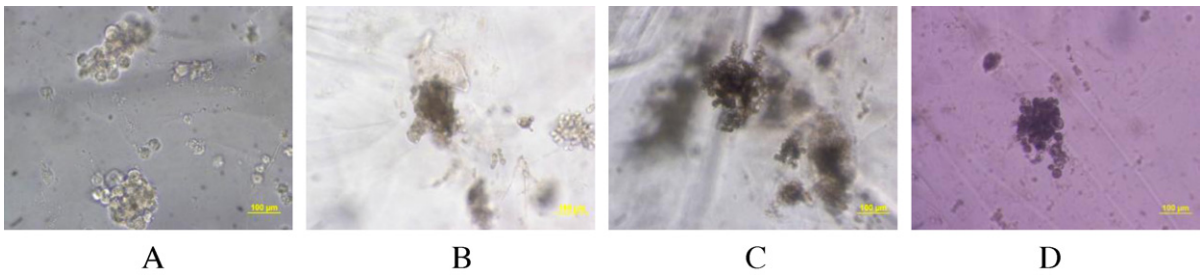

Fig. 5. Optical microscope images of HO8910 cells cultured in the Gel-2 hydrogels on 5th–20th day. A 5th day; B 10th day; C 15th day; D 20th day.

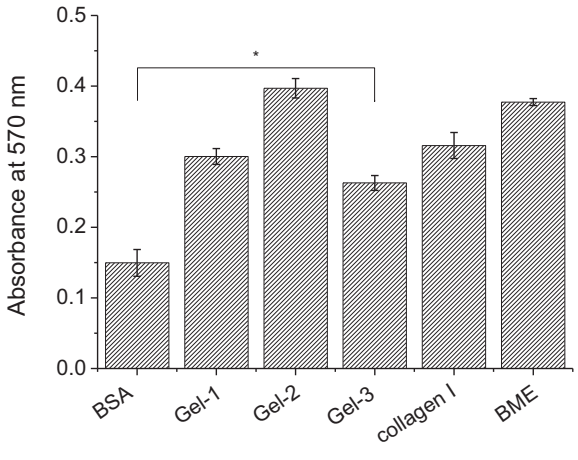

Fig. 6. The adhesion of HO8910 on Gel-1, Gel-2, Gel-3, collagen I, and BME hydrogel.

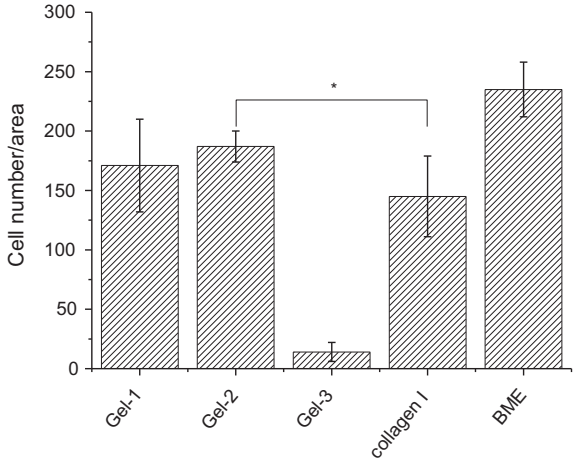

Fig. 8. The migration and invasion of HO8910 cells through Gel-1, Gel-2, Gel-3, collagen I, and BME hydrogel.

these synthesized hydrogel matrices possess some biological functionality similar to collagen I or BME hydrogel and facilitate the maintenance of the malignant phenotypes of human ovarian cancer cells or the high invasion potentials.

Hydrogel Gel-1 and Gel-2 not only show the better HO8910 cells adhesion capability, but also can allow the cells to migrate and invade through hydrogel layer while hydrogel Gel-3 limited the migration of ovarian cells to some extent. Fig. 8 illustrated the comparison of migration of HO8910 cells in five different hydrogels. Gel-1, Gel-2 and collagen I performed the similar cell migration, BME is the best while Gel-3 can not well support the migration of HO8910 cells. The micro-scale porous structure can not be observed in hydrogel microparticles. So ovarian cancer cells with the size of some 10 μm can not migrate through mesh of hydrogel, but gap

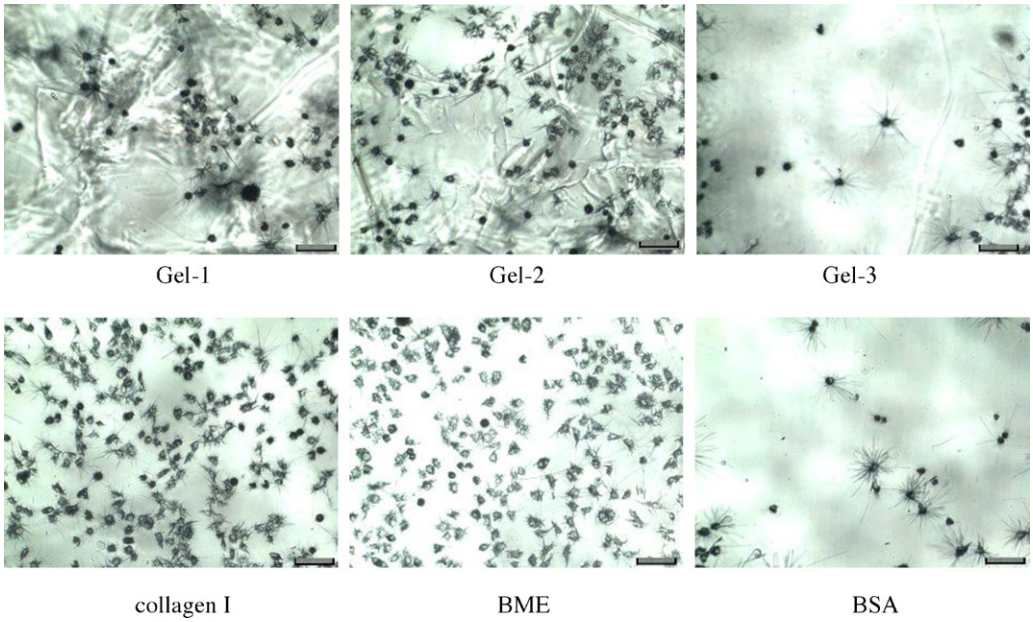

Fig. 7. The optical microscope images of adhered HO8910 cells on Gel-1, Gel-2, Gel-3, collagen I, and BME hydrogel layer. (All images were captured at ×100 magnification; Scale bar: 100 μm).

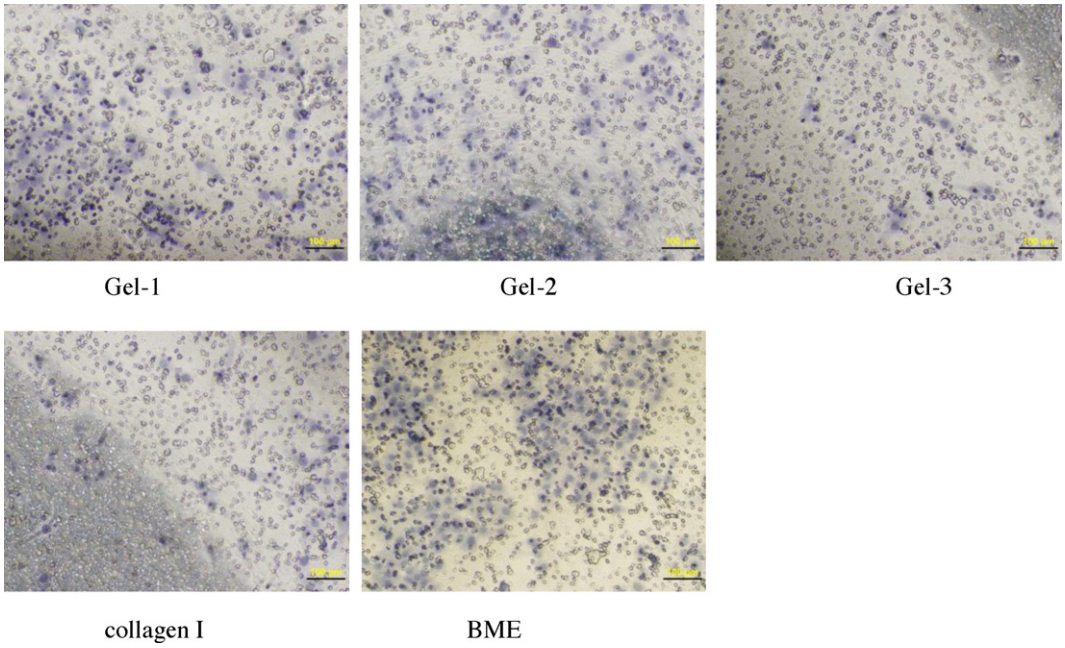

Fig. 9. Optical microscope images of migrated HO8910 cells through Gel-1, Gel-2, Gel-3, collagen I, and BME hydrogel to PCF membrane. (All images were captured at ×100 magnification; Scale bar: 100 μm).

among the separate pieces of hydrogel. The possible reason is that the gap among microgels with the higher with higher storage modulus is larger; therefore the cells can migrate through these gaps, while the gap among hydorgel pieces with lower storage modulus possibly is smaller and therefore prevent the migration of cells. The cells migration activity in Gel-1, Gel-2 is better than that in collagen I, but is lower than that in BME hydrogel.

Fig. 9 shows the number of captured HO8910 cells (blue area) on the PCF membrane after migrated through the different hydrogel layers. The number of captured cells on the PCF membrane after migrated through Gel-2 or Gel-1 ranges from 150 to 190, which is much larger than the number of captured cells on the PCF membrane after migrated through Gel-3.

The adhesion, migration and invasion assay of Gel-1, Gel-2, and Gel-3 indicate that the better adhesion capability is, the better the proliferation viability of ovarian cancer cells is. The better migration and invasion capability in hydrogel equally contribute to the formation and growth of multicellular spheroid. As shown in Fig. 5, the MCS was not only formed on the hydrogel Gel-2, but also formed within the hydrogel Gel-2, which indicates directly that the favorable cells adhesion and migration capabilities are the essential preconditions of cell proliferation in hydrogel. The different migration behaviors of ovarian cancer cell HO9810 in this kind of un-degradable hydrogel with different elastic modulus imply that the ovarian cancer cells are possibly more apt to migrate through the porous or unrepaired wall of blood vessels *in vivo*.

4. Conclusion

In conclusion, poly(ethylene glycol)-cross linked poly(methyl vinyl ether-*co*-maleic acid) (PMVE-*co*-MA) hydrogel is cytocompatible and non-thermoresponsive, which can be used potentially a new type of cell culture matrix, the response of ovarian cancer cell lines HO8910 to the mechanical properties of this hydrogel is very different. Preliminary cell culture results proved that this kind of hydrogel is preferable to support proliferation and the formation of multicellular spheroids of ovarian cancer cells HO8910 in a 3D model if the mechanical properties of hydrogel are appropriate. The proliferation of HO8910 cells can last up to 15 days. The mechanical properties of hydrogel depending on the crosslinking degree play a critical role in cell growth. The hydrogel with the higher elastic modulus can lead to the successful 3D proliferation of HO8910 cells and the formation of MCS, at the same time, also can support well the adhesion, migration and invasion of cells. In contrast, the hydrogel with the lower elastic modulus can not become the matrix for 3D culture. This synthesized hydrogel model provide the important biological activities similar to collagen I and BME for ovarian tumorigenesis, metastasis, and colonization in 3D culture model. The above research results also suggest that the nature of hydrogel composition is not only very important but also the mechanical properties of hydrogel are equally critical for cell behaviors in 3D cell culture. The further study is still in progress.

Acknowledgements

We acknowledge the support of the National Basic Research Program of China (2011CB933503), the program for New Century Excellent Talents in University (NCET-09-0298), the Special Project on Development of National Key Scientific Instruments and Equipment of China (2011YQ03013403), National Natural Science Foundation of China (61179035), and Suzhou Applied Basic Research Fund (SYG201003). The author also would like to thank Dr. Yan Huang for FT-IR spectra measurements.

References

[1] A. Nyga, U. Cheema, M. Loizidou, 3D tumour models: novel in vitro approaches to cancer studies, J. Cell Commun. Signal. 5 (2011) 239–248.
[2] R.-Z. Lin, H.-Y. Chang, Recent advances in three-dimensional multicellular spheroid culture for biomedical research, Biotechnol. J. 3 (2008) 1172–1184.
[3] X. Zhang, W. Wang, W. Yu, Y. Xie, X. Zhang, Y. Zhang, X. Ma, Development of an in vitro multicellular tumor spheroid model using microencapsulation and its application in anticancer drug, Biotechnol. Prog. 21 (2005) 1289–1296.
[4] S.R. Khetani, S.N. Bhatia, Microscale culture of human liver cells for drug development, Nat. Biotech. 26 (2007) 120–126.
[5] D.W. Hutmacher, Biomaterials offer cancer research the third dimension, Nat. Mater 9 (2009) 90–93.
[6] L. Besseau, B. Coulomb, C. Lebreton-Decoster, M.-M. Giraud-Guille, Production of ordered collagen matrices for three-dimensional, Biomaterials 23 (2002) 27–36.

[7] H.K. Dhiman, A.R. Ray, A.K. Panda, Characterization and evaluation of chitosan matrix for in vitro growth of MCF-7 breast cancer cell lines, Biomaterials 25 (2004) 5147–5154.
[8] J.A. Rowley, G. Madlambayan, D.J. Mooney, Alginate hydrogels as synthetic extracellular matrix materials, Biomaterials 20 (1999) 45–53.
[9] B. Grun, E. Benjamin, J. Sinclair, J.F. Timms, I.J. Jacobs, S.A. Gayther, D. Dafou, Three-dimensional in vitro cell biology models of ovarian and endometrial cancer, Cell Prolif. 42 (2009) 219–228.
[10] V.M. Weaver, S. Lelièvre, J.N. Lakins, M.A. Chrenek, J.C.R. Jones, F. Giancotti, Z. Werb, M.J. Bissell, Beta4 integrin-dependent formation of polarized three-dimensional architecture confers resistance to apoptosis in normal and malignant mammary epithelium, Cancer Cell 2 (2002) 205–216.
[11] A. Khademhosseini, G. Eng, J. Yeh, J. Fukuda, J. Blumling III, R. Langer, J.A. Burdick, Micromolding of photocrosslinkable hyaluronic acid for cell encapsulation and entrapment, J. Biomed. Mater. Res. A 79 (2006) 522–532.
[12] L.-S. Wang, J.E. Chung, P.P.-Y. Chan, M. Kurisawa, Injectable biodegradable hydrogels with tunable mechanical properties for the stimulation of neurogenesic differentiation of human mesenchymal stem cells in 3D culture, Biomaterials 31 (2010) 1148–1157.
[13] M.C. Cushing, K.S. Anseth, Hydrogel cell cultures, Science 316 (2007) 1133–1134.
[14] K. Shield, M.L. Ackland, N. Ahmed, E.G. Rice, Multicellular spheroids in ovarian cancer metastases: biology and pathology, Gynecol. Oncol. 113 (2009) 143–148.
[15] J. Friedrich, C. Seidel, R. Ebner, L.A. Kunz-Schughart, Spheroid-based drug screen: considerations and practical approach, Nat. Protocols 4 (3) (2009) 309–324.
[16] J.D. Hartgerink, E. Beniash, S.I. Stupp, Peptide-amphiphile nanofibers: a versatile scaffold for the preparation of self-assembling materials, Proc. Natl. Acad. Sci. USA 99 (2002) 5133–5138.
[17] V. Jayawarna, S.M. Richardson, A.R. Hirst, N.W. Hodson, A. Saiani, J.E. Gough, R.V. Ulijn, Introducing chemical functionality in Fmoc-peptide gels for cell culture, Acta Biomaterialia 5 (2009) 934–943.
[18] Z. Yang, X. Zhao, A 3D model of ovarian cancer cell lines on peptide nanofiber scaffold, Int. J. Nanomed. 5 (2011) 303–310.
[19] M. Ehrbar, S.C. Rizzi, R.G. Schoenmakers, B.S. Miguel, J.A. Hubbell, F.E. Weber, M.P. Lutolf, Biomolecular hydrogels formed and degraded via site-specific enzymatic reactions, Biomacromolecules 8 (2007) 3000–3007.
[20] D. Loessner, K.S. Stok, M.P. Lutolf, D.W. Hutmacher, J.A. Clements, S.C. Rizzi, Bioengineered 3D platform to explore cell-ECM interactions and drug resistance of epithelial ovarian cancer cells, Biomaterials 31 (2010) 8494–8506.
[21] A.M. Kloxin, C.J. Kloxin, C.N. Bowman, K.S. Anseth, Mechanical properties of cellularly responsive hydrogels and their experimental determination, Adv. Mater. 22 (2010) 3484–3494.
[22] W. Xu, R. Mezencev, B. Kim, L. Wang, J. McDonald, T. Sulchek, Cell stiffness is a biomarker of the metastatic potential of ovarian cancer cells, PLoS One 7 (10) (2012) e46609.
[23] T.R. Raj Singh, A.D. Woolfson, R.F. Donnelly, Investigation of solute permeation across hydrogels composed of poly(methyl vinyl ether-co-maleic acid) and poly(ethylene glycol), J. Pharm. Pharmacol. 62 (2010) 829–837.
[24] T.R.R. Singh, P.A. McCarron, A.D. Woolfson, R.F. Donnelly, Investigation of swelling and network parameters of poly(ethylene glycol)-cross linked poly(methyl vinyl ether-co-maleic acid) hydrogels, Eur. Polym. J. 45 (2009) 1239–1249.
[25] B.J. Gill, D.L. Gibbons, L.C. Roudsari, J.E. Saik, Z.H. Rizvi, J.D. Roybal, J.M. Kurie, J.L. West, A synthetic matrix with independently tunable biochemistry and mechanical properties to study epithelial morphogenesis and EMT in a lung adenocarcinoma model, Cancer Res. 7 (22) (2012) 6013–6023.
[26] D. Wang, D. Cheng, Y. Guan, Y. Zhang, Thermoreversible hydrogel for inSitu generation and release of HepG2 spheroid, Biomacromolecules 12 (2011) 578–584.